

On plasma detachment in propulsive magnetic nozzles

Eduardo Ahedo^{a)} and Mario Merino

E.T.S. Ingenieros Aeronáuticos, Universidad Politécnica de Madrid, Madrid 28040, Spain

(Received 1 February 2011; accepted 6 April 2011; published online 27 May 2011)

Three detachment mechanisms proposed in the literature (via resistivity, via electron inertia, and via induced magnetic field) are analyzed with an axisymmetric model of the expansion of a small-beta, weakly collisional, near-sonic plasma in a diverging magnetic nozzle. The model assumes cold, partially magnetized ions and hot, isothermal, fully magnetized electrons. Different conditions of the plasma beam at the nozzle throat are considered. A central feature is that a positive thrust gain in the nozzle of a plasma thruster is intimately related to the azimuthal current in the plasma being diamagnetic. Then, and contrary to existing expectations, the three aforementioned detachment mechanisms are divergent, that is, the plasma beam diverges outwards of the guide nozzle, further hindering its axial expansion and the thrust efficiency. The rate of divergent detachment is quantified for the small-parameter range of the three mechanisms. Alternative mechanisms for a convergent detachment of the plasma beam are suggested. © 2011 American Institute of Physics. [doi:10.1063/1.3589268]

I. INTRODUCTION

A diverging magnetic nozzle, created by a longitudinal magnetic field, is being proposed as an acceleration mechanism for a magnetized plasma in advanced propulsion devices, such as the helicon thruster,¹⁻⁴ the Applied-Field MagnetoPlasmaDynamic Thruster (AFMPDT),⁵ the Diverging Cusped Field Thruster (DCFT),⁶ and the VArIable Specific Impulse Magneto Rocket (VASIMR).⁷ In particular, the magnetic nozzle constitutes the acceleration stage of the helicon thruster, located downstream of the chamber where the plasma is created and heated. The plasma flow, channeled by the diverging magnetic lines, expands supersonically in a similar way to a hot gas in a solid nozzle.⁸ Beyond this basic analogy, conventional gas dynamics in a solid nozzle are much simpler than plasma dynamics in a magnetic nozzle.

In order to understand these ones, we developed a macroscopic, two-dimensional (2D) model of the stationary expansion of a plasma with fully magnetized, hot electrons and partially magnetized, cold ions, in the diverging magnetic nozzle created by solenoids.⁹ Plasma conditions at the nozzle throat include sonic and supersonic flows, and radially non-uniform or uniform profiles of the beam density. The model consists of a closed set of conservation and differential equations which are integrated efficiently with the method of characteristic surfaces. The model includes several relevant design/operation parameters, which allowed our analysis to go beyond the simulation of some particular cases, into investigating the influence of an ample region of the parametric space in the plasma response. The model was designed specifically to analyze plasma acceleration in an helicon thruster, due to the conversion of electron thermal energy into ion directed energy. It could be partially suitable for the AFMPDT and the DCFT, but the detailed physics of these devices are not understood enough yet. The model is

not apt for studying plasma acceleration in the VASIMR nozzle, caused by conversion of ion gyrokinetic energy into nozzle parallel energy.

Since the nozzle magnetic lines close on themselves, once the plasma beam has been accelerated and before the turning point of the magnetic nozzle, the plasma jet needs to detach from the magnetic lines; otherwise, part of the plasma would turn back towards the thruster walls and the thrust gain will drop. Experiments seem to suggest that most of the plasma detaches, but more measurements are needed and detachment mechanisms is poorly known. In this context and in order to optimize the design of magnetic nozzles for plasma thrusters, one crucial subject is to understand how the plasma detaches from the magnetic nozzle. Three detachment mechanisms of the plasma from the guide magnetic field have been proposed in the literature: resistive detachment by Moses *et al.*,¹⁰ electron-inertia detachment by Hooper,¹¹ and magnetic self-field detachment by Arefiev and Breizman¹² and Breizman *et al.*¹³ In the two first cases, either resistive or electron-inertia forces detach the plasma jet from the guide field nozzle. In the third case, the induced magnetic field modifies the original nozzle of the guide field; the plasma, by remaining attached to the resulting magnetic nozzle, detaches effectively from the guide field. The three detachment studies either obtain or assume that the detachment is *convergent*, i.e., the plasma beam diverges less than the guide field nozzle, thus facilitating the axial plasma expansion.

This paper analyzes these three detachment mechanisms, both qualitatively and quantitatively (in the small-parameter range), computing perturbed quantities from the 2D solution for a collisionless, zero-beta plasma with massless electrons. Several observations related to the frame of our study are worth to comment. First, as the title announces, the detachment assessment is going to be centered in the case of a *propulsive magnetic nozzle* (PMN), of which nozzle's main role is to enhance the thrust by acceleration of a near-sonic

^{a)}Electronic mail: eduardo.ahedo@upm.es.

plasma and conversion of its internal energy into directed kinetic energy. The PMN is not the case treated by Hooper and Arefiev and Breizman, who consider a plasma that is already hypersonic at the nozzle entrance; in fact, Arefiev and Breizman report a decrease of the axial flux of plasma momentum along the nozzle, i.e., a thrust loss. Second, although detachment is expected to manifest mainly after the plasma has been accelerated, both processes are not independent and well separated in the nozzle; thus, it is preferable to analyze them within a unique model.

The rest of the paper is organized as follows. Section II reviews succinctly the PMN model and the relation between plasma currents and the thrust increment. Section III analyzes resistive and electron-inertia detachment. Section IV is devoted to magnetic detachment. Conclusions and ideas for further research are presented in Sec. V. First results on this subject were presented in a recent conference.¹⁴

II. THRUST GAIN AND PLASMA CURRENTS

The plasma/nozzle model and the nomenclature used hereafter are exactly the same ones of Ref. 9, so we will omit their description as far as comprehension of the present work is not affected. A current-free, fully ionized plasma jet of radius R , is injected sonically at the throat (located at $z = 0$) of a nozzle created by a guide magnetic field of strength B . The plasma at the throat satisfies

$$\lambda_{d0} \ll \ell_{e0} \ll R, \quad \Omega_{i0}R/u_{i0} = O(1), \quad (1)$$

$$m_e/m_i \ll 1, \quad R/\lambda_{ei0} \ll 1, \quad \beta_0 \equiv \mu_0 n_0 T_e / B_0^2 \ll 1, \quad (2)$$

where subscript 0 refers always to values at $(z, r) = (0, 0)$, R is the radius of the plasma jet at $z = 0$, n is the plasma density, u_i is the macroscopic ion longitudinal velocity, λ_d is the Debye length, ℓ_e is the electron gyroradius, λ_{ei} is the electron-ion collision mean-free-path, $\Omega_i = eB/m_i$ is the ion gyrofrequency, and the rest of symbols are conventional. Table I of Ref. 9, detailing parameters of two helicon thruster experiments,^{2,3} shows that conditions (1) and (2) are appropriate for studying the plasma discharge in those thrusters. Then, we can consider that the plasma is collisionless and quasineutral, electrons are massless and fully magnetized, ions are mildly magnetized, and the induced magnetic field B^* is negligible. Electron streamtubes are the magnetic streamtubes, but ion streamtubes do not coincide with electron streamtubes, except at the jet axis and edge $r = R_V(z)$ (see Fig. 6 of Ref. 9).

Reference 9 is centered on the zero asymptotic limit of the parameters of Eq. (2). Then, the plasma expansion model consists of Eqs. (20)–(22) and (24)–(27), which determine the ion and electron velocities, \mathbf{u}_i and \mathbf{u}_e , plasma density n , and electric potential ϕ . The upstream boundary conditions for these equations are Eqs. (29)–(35) of Ref. 9. Downstream, the integration cannot proceed beyond the turning point of the magnetic tube containing the plasma jet. This forces us to limit our study to a finite axial section downstream of the nozzle.

An exam of the equations shows that the plasma/nozzle model is characterized by the divergence rate of the mag-

netic topology (parameter R_L/R for a single loop in Ref. 9); $\hat{\Omega}_{i0} = \Omega_{i0}R/c_s$, measuring the magnetic strength (on ions); $M_0 = u_{i0}/c_s$, the ion Mach number at the throat, with $c_s = \sqrt{T_e/m_i}$ the plasma sound speed; and σ , measuring the non-uniformity of $n(z=0, r)$ in Eq. (33) of Ref. 9. At least for an helicon thruster, the plasma at the nozzle throat is expected to be highly non-uniform ($\sigma \approx 1$), quasi-sonic ($M_0 \approx 1$), and ions to be weakly magnetized ($\hat{\Omega}_{i0} \leq 1$).^{15,16} These entrance conditions are very different from the ones considered by Arefiev and Breizman¹² and Breizman *et al.*¹³: a plasma which is radially uniform ($\sigma = 0$), cold ($M_0 \rightarrow \infty$), and strongly magnetized ($\hat{\Omega}_{i0} \rightarrow \infty$). Leaving aside the relevance of the Arefiev-Breizman model for a propulsive nozzle, these two disparate parametric ranges provide a good opportunity to understand how thrust gain and detachment depend on the upstream plasma conditions. We will approach Arefiev-Breizman conditions by taking $\hat{\Omega}_{i0}$ and M_0 large but finite; for instance, for $M_0 = 3$, the plasma is almost hypersonic, since the influence of the plasma pressure on the nozzle expansion is reduced to about a 10%.

According to Eqs. (40)–(42) of Ref. 9, the accumulated thrust gain at a cross-section $S_z : z = \text{const}$ is measured by the dimensionless function

$$\kappa_{noz}(z) = \Delta F(z)/F_0, \quad (3)$$

where $F = F(0)$ is the momentum axial flux of the plasma at $z = 0$ and

$$\Delta F(z) = \int_{\mathcal{V}(z)} dV (-j_\theta) B_r + \int_{A_V(z)} dA (-J_\theta) B_r \quad (4)$$

is the gain in momentum axial flux, with $\mathcal{V}(z)$ and $A_V(z)$ the volume and area of the region bounded by the nozzle throat, the section S_z , and the plasma/vacuum edge V . Thus, the increase of momentum flux of the plasma beam along the nozzle is due to the axial magnetic force exerted by the thruster magnetic circuit on the volumetric and superficial azimuthal currents, j_θ and J_θ respectively, induced on the plasma. Since the supersonic fluid information travels only downstream, $\kappa_{noz}(z)$ represents the thrust gain for a nozzle of length z .

Without loss of generality, the convention $B_r, B_z > 0$ is adopted in the model. Then, Eq. (4) states that a positive thrust gain requires the azimuthal electric current be negative, which, as we will see below, corresponds to a diamagnetic current. The superficial current J_θ , due to pressure gradients at the plasma edge, is negative always. The current density $j_\theta = j_{\theta i} + j_{\theta e}$ has ion and electron contributions (called, respectively, *swirl* and *Hall* currents¹⁷), which, respectively, are positive and negative.⁹ Therefore, the Hall current accelerates the plasma and the swirl current decelerates it.

Sketches of the two physical arrangements of plasma currents are shown in Figs. 1(a) and 1(b). They show the azimuthal currents in the magnetic circuit and in the plasma plume (either internal or at the edge). These two sets of currents create, respectively, the applied magnetic field, \mathbf{B} , and the plasma-induced magnetic field, \mathbf{B}^* . The Ampere's law for the longitudinal (main) component of the induced field is

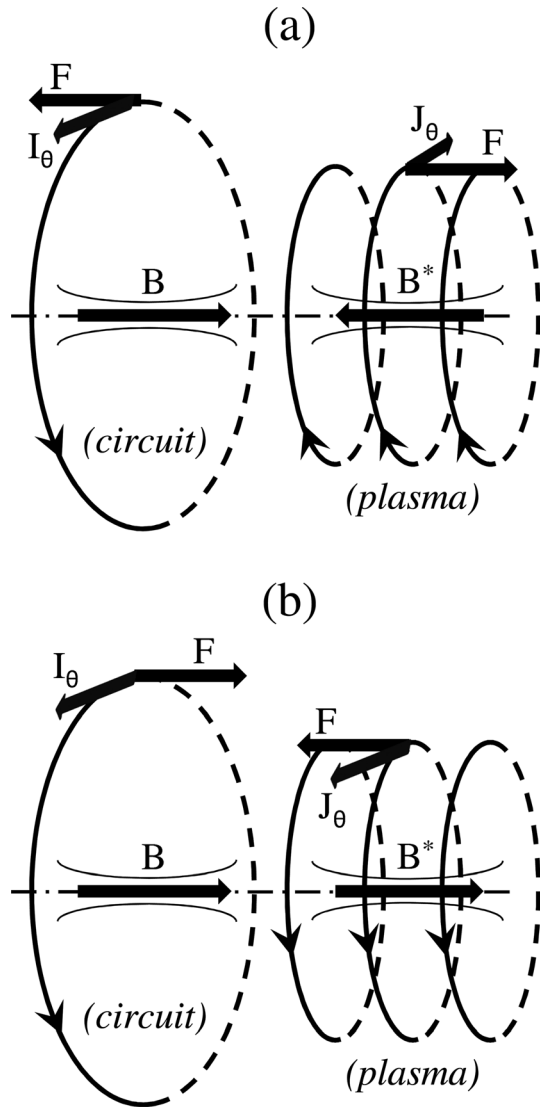


FIG. 1. Sketches of the azimuthal currents in the external circuit and the plasma beam, the magnetic fields they create, and the mutual force between them. (a) Diamagnetic case, corresponding to plasma acceleration and positive thrust gain in the nozzle, the suitable configuration for a plasma thruster. (b) Paramagnetic case, corresponding to plasma deceleration and negative thrust gain.

$$\nabla \times \tilde{\mathbf{B}}^* = \mu_0 j_\theta \mathbf{1}_\theta. \quad (5)$$

Two sets of parallel currents repel or attract each other, with the mediation of the magnetic fields they create, depending on whether they run in the opposite or the same direction, respectively.¹⁸ The case of mutual repulsion, shown in Fig. 1(a), is the suitable one for a PMN: the plasma current is pushed downstream and the circuit current (tied to the thruster) is pushed back, thus yielding a positive thrust gain. The case of the mutual attraction, sketched in Fig. 1(b), leads to plasma deceleration and $\kappa_{noz} < 0$.

The thrust gain for cases with $M_0 = 1.05$ and $M_0 = 3$ is plotted in Fig. 2(a). For the simplest case of an initially uniform plasma with unmagnetized ions, κ_{noz} behaves similarly to the case of a conventional gas in a solid nozzle: κ_{noz}

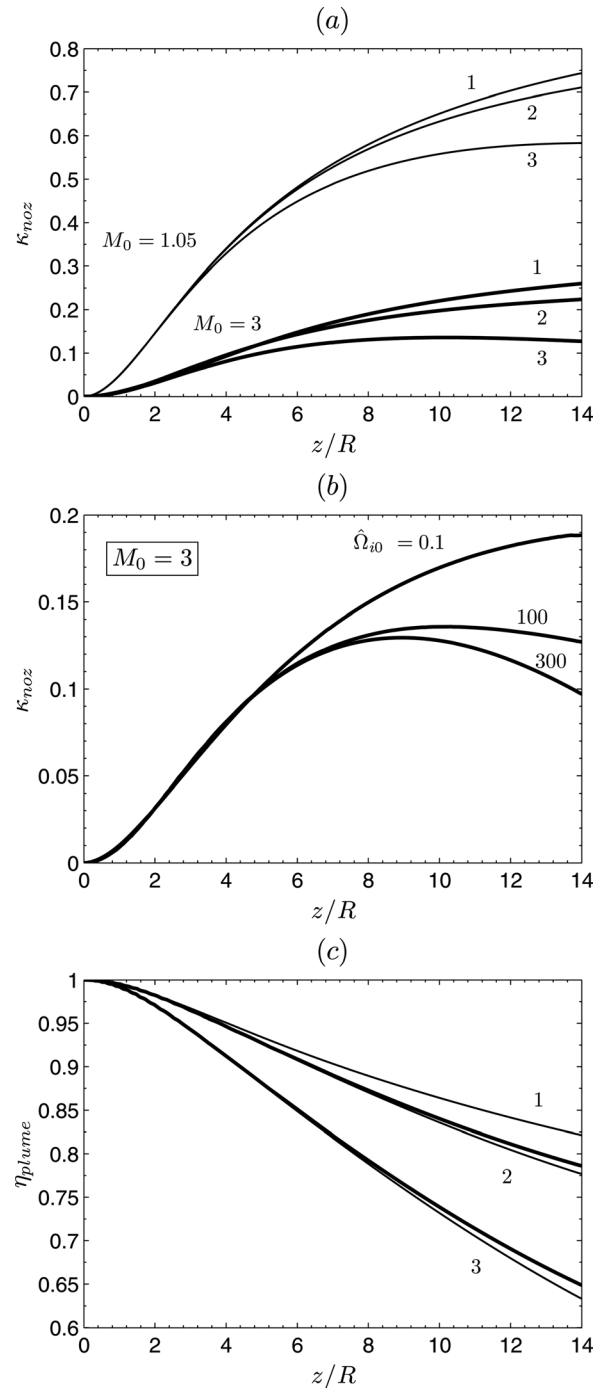


FIG. 2. (a) Comparison of the thrust gain for $M_0 = 1.05$ (thin lines) and $M_0 = 3$ (thick lines). Numbers (1)–(3) indicate $\hat{\Omega}_{i0} = 0.1$, $\sigma = 0.99$; $\hat{\Omega}_{i0} = 100$, $\sigma = 0.99$; and $\hat{\Omega}_{i0} = 100$, $\sigma = 0$, respectively. (b) Influence of the magnetic field strength on the thrust gain for $M_0 = 3$. (c) Plume efficiency versus the nozzle length for $M_0 = 1.05$. Lines and numbers are as in plot (a). In all figures, simulations are for the large divergence-rate nozzle of Ref. 9.

depends on the ratio on the electron-to-ion momentum flux ratio, which is highest for $M_0 = 1$ and is zero for a hypersonic plasma. Figure 2(a) shows that κ_{noz} is about 3 times lower for $M_0 = 3$ than for $M_0 \approx 1$, and $\kappa_{noz} \rightarrow 0$ is expected for a cold plasma. With respect to the other two parameters, κ_{noz} increases when either σ increases (which augments the positive Hall current) or $\hat{\Omega}_{i0}$ decreases (which reduces the

negative swirl current). Both effects are observed in Fig. 2(a) too.

Since the swirl current is found negligible in the plasma source¹⁵ and develops almost exclusively along the nozzle (because of the separation of magnetic and ion streamtubes), its negative effect on thrust increases as the plasma moves downstream. As a consequence, $\kappa_{noz}(z)$ can reach a maximum at a certain distance from the throat. This is clearly observed in Fig. 2(b): for $M_0 = 3$ and $\hat{\Omega}_{i0} = 300$, the thrust gain is maximum for $z/R \approx 9$, and the swirl current is larger than the Hall current downstream of that location.

In the limit case of $\hat{\Omega}_{i0} \gg 1$ and $M_0 \gg 1$, the Hall current is negligible [see Eqs. (24) and (25) of Ref. 9] and the paramagnetic, decelerating swirl current leads to $\kappa_{noz}(z) < 0$. Indeed, Arefiev and Breizman define a “nozzle efficiency” (based on thrust) that is similar to $1 + \kappa_{noz}$, which is plotted in Fig. 6 of Ref. 13; losses up to $-\kappa_{noz} \sim 38\%$ are shown. The sketch of Fig. 4 of Ref. 12 corresponds to the one in Fig. 1(b) here. The “nozzle efficiency” of Arefiev and Breizman must not be mistaken with the plume efficiency of Ref. 9, $\eta_{plume}(z) = P_{zi}/P_i$, where P_{zi} and P_i are the axial and total fluxes of ion energy at section S_z , defined in Eqs. (44) and (47) of Ref. 9. The plume efficiency is a genuine 2D effect that measures the penalty in thrust efficiency caused by the beam radial expansion. Figure 2(c) shows that η_{plume} is weakly influenced by M_0 . As the thrust gain, the plume efficiency is higher for a non-uniform jet with unmagnetized ions, since this presents the lowest (effective) divergence.⁹

III. DIFFUSIVE DETACHMENT

Each one of the three detachment mechanisms proposed in the literature is due to one of the small parameters of Eq. (2). In this section and Sec. IV, these mechanisms are studied in the small-parameter limit, assuming that the plasma response is the sum of the zeroth-order (attached) solution plus a first-order solution. This one isolates each detachment phenomenon, determines its character, and quantifies it (up to first order).

Diffusive detachment considers that the plasma detaches from the magnetic lines by either resistive¹⁰ or inertial¹¹ forces on electrons. The key equation for diffusive detachment is the one for electron azimuthal momentum which, including resistivity and inertia, becomes

$$eu_{\perp e}B = (m_e/r)\tilde{\mathbf{u}}_e \cdot \nabla(ru_{\theta e}) + m_e\nu_{ei}u_{\theta e}, \quad (6)$$

with $\nu_{ei} \equiv c_s/\lambda_{ei}$, the Coulomb collision frequency. The massless and collisionless, zeroth-order solution reduces Eq. (6) to $u_{\perp e} = 0$. The first-order solution of $u_{\perp e}$ is obtained by implementing the zeroth-order solution on the right-hand side of Eq. (6). Using Eq. (25) of Ref. 9, the inertial contribution to Eq. (6) becomes $\tilde{\mathbf{u}}_e \cdot \nabla(ru_{\theta e}) = 2u_{\theta e}u_{re}$, with $u_{re} = u_{\parallel e} \sin \alpha$ and α , the local angle of \mathbf{B} with respect to the plasma axis. Thus, the perpendicular velocity satisfies the algebraic relation

$$u_{\perp e} = \bar{\chi}u_{\theta e}, \quad (7)$$

where the *inverse Hall parameter*, $\bar{\chi} = \bar{\chi}_{res} + \bar{\chi}_{ine}$, has contributions from resistivity and electron inertia,

$$\bar{\chi}_{res} = \nu_{ei}/\Omega_e, \quad \bar{\chi}_{ine} = 2u_{re}/r\Omega_e, \quad (8)$$

and

$$\Omega_e = \Omega_i m_e/m_i.$$

Two conclusions are straightforward from Eqs. (7) and (8). First, electron-inertia effects have a resistive character with an effective collision frequency $2u_{re}/r \geq 0$; thus, the ratio $2u_{re}/(r\nu_{ei})$ determines which one is the main diffusive phenomenon. Second, the ratio $u_{\perp e}/u_{\theta e}$ is positive always. Since a PMN has $u_{\theta e} \geq 0$ (with convention $B_z > 0$), one has $u_{\perp e} \geq 0$, and diffusion (either resistive or inertial) makes the plasma beam to detach *divergently*. This result disagrees with Hooper,¹¹ who claimed that electron inertia leads to convergent detachment. Hooper’s model is limited to a hypersonic, uniform plasma beam at the nozzle throat and assumes that current ambipolarity is fulfilled everywhere. Reference 9 demonstrates that current ambipolarity is not satisfied, so the disagreement on the character of the diffusive detachment is very likely motivated on that assumption.

The rate of diffusive detachment is measured by the ratio

$$\delta = u_{\perp e}/u_{\parallel e} = \bar{\chi}u_{\theta e}/u_{\parallel e} = \delta_{res} + \delta_{ine}, \quad (9)$$

with

$$\delta_{res} = \frac{\nu_{ei}u_{\theta e}}{\Omega_e u_{\parallel e}}, \quad \delta_{ine} = \frac{2u_{\theta e} \sin \alpha}{r\Omega_e}, \quad (10)$$

as the detachment rates for resistivity and electron-inertia. Figure 3 illustrates the behavior of resistive detachment for a typical PMN case. The normalization parameters for the inverse Hall parameter and the detachment rate are

$$\delta_{res,0}\hat{\Omega}_{i0} \equiv \bar{\chi}_{res,0} = \hat{\nu}_{ei0}/\hat{\Omega}_{e0},$$

with $\hat{\Omega}_{e0} = \hat{\Omega}_{i0}m_e/m_i$; typical values of $\bar{\chi}_{res,0}$ (as for the plasmas of Table I of Ref. 9) are in the range $10^{-4} - 10^{-3}$. Except near the plasma edge, where rarefaction is enhanced, one has $\bar{\chi}_{res} \propto n/B \propto 1/M$ and $\delta_{res} \propto Rv/M^2$, which explains that $\delta_{res}\delta_{res,0} \ll 1$ everywhere. Therefore, resistive detachment is expected to be negligible in practical PMNs. Moses *et al.*¹⁰ suggest that anomalous resistivity or electron cooling could increase the effective collision frequency. Some observations are pertinent. First, this will further increase divergent detachment. Second, as far as we know, there is not experimental evidence of anomalous diffusion in magnetic nozzles. And third, although some electron cooling is known to exist, it is unlikely that ν_{ei} increases by even one order of magnitude.

Figure 4 illustrates inertia-based detachment for the same zeroth-order conditions than Fig. 3. Now, the normalization parameters are

$$\delta_{ine,0}\hat{\Omega}_{i0} \equiv \bar{\chi}_{ine,0} = 2/\hat{\Omega}_{e0}$$

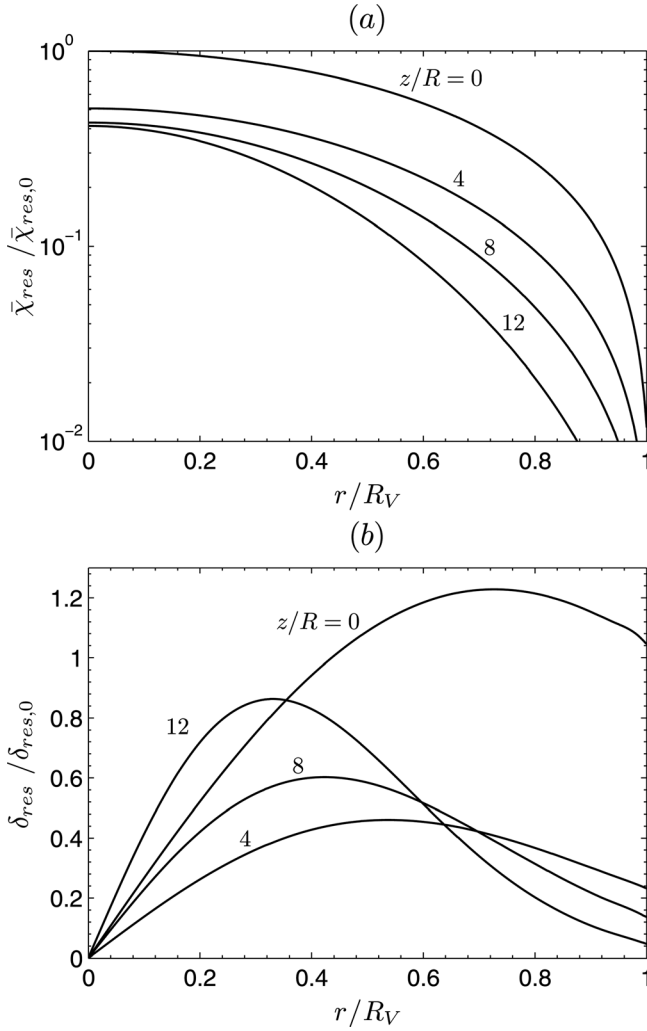


FIG. 3. Resistive detachment for $M_0 = 1.05$, $\sigma = 0.99$, and $\hat{\Omega}_0 = 0.1$. (a) Inverse Hall parameter and (b) divergent detachment slope.

with $\bar{\chi}_{ine,0} \sim 10^{-5} - 10^{-4}$, typically. Except near the plasma edge, it is $\bar{\chi}_{ine} \propto MR_V \sin \alpha$ and $\delta_{ine} \propto R_V^2 \sin \alpha$. Contrary to resistivity, inertial detachment increases considerably as the plasma moves downstream and u_{re} develops. Additionally δ_{ine} increases at $r/R_V \sim 1$ because of the sharp increase of $u_{\theta e}$ near the plasma-vacuum edge.⁹ For the envisaged range of parameters for a PMN, electron-inertia effects yield a larger divergent detachment than resistivity. Although $\delta_{ine,0} \ll 1$, the large values of $\delta_{ine} / \delta_{ine,0}$ suggest that inertial detachment can become a zeroth-order effect downstream, unless that non-linear effects in Eq. (6) prevent it, as we discuss below.

Diffusive detachment is based on the electron response exclusively; in particular, on the development of a Hall current that balances (partially or totally) the pressure gradient. Therefore, this detachment is divergent even for a supersonic plasma at the nozzle throat. Furthermore, we can interpret the outwards diffusion in the nozzle as the continuation of the one that takes place inside a cylindrical plasma source^{15,16}: the radially outwards flux of a plasma constrained by an axial magnetic field and a cylindrical vessel is made possible by (1) plasma resistivity in the bulk plasma region and (2) electron-inertia in a thin inertial layer, separat-

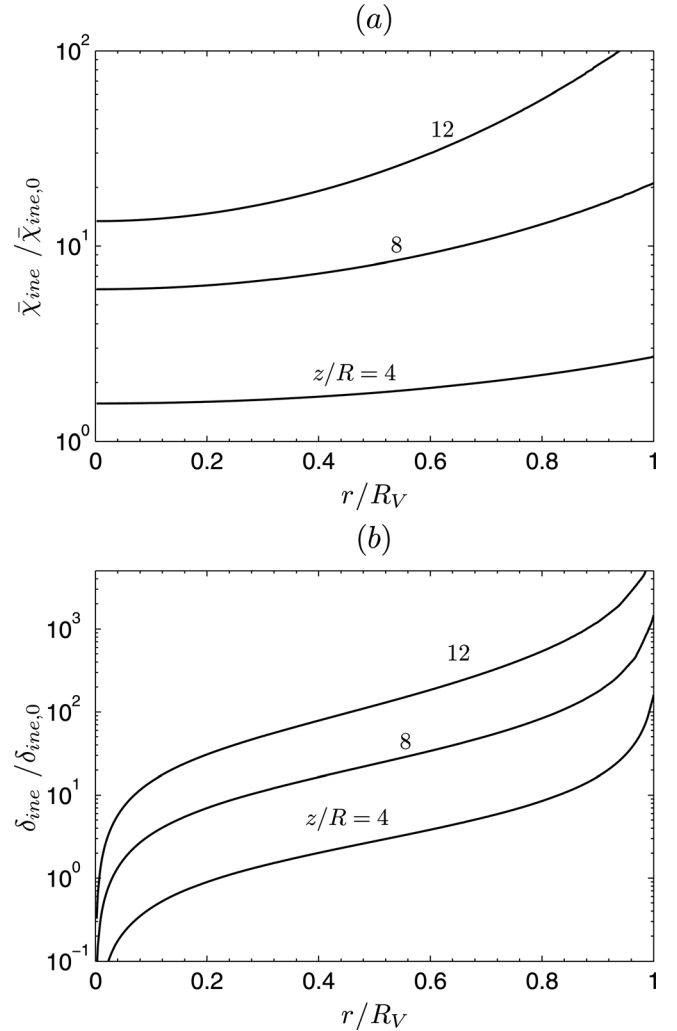


FIG. 4. Electron-inertia detachment for $M_0 = 1.05$, $\sigma = 0.99$, and $\hat{\Omega}_0 = 0.1$. (a) Inverse Hall parameter and (b) divergent detachment slope.

ing the bulk region and the Debye sheath. The continuation of the inertial and Debye layers into the nozzle would occupy the regions here named plasma edge and vacuum (although their study is out of the present model capabilities). In our model, the plasma injected at the nozzle throat corresponds only to the bulk region; the large increment of $u_{\theta e}(0, r)$ near the beam edge, Eq. (34) of Ref. 9, announces the presence of the inertial layer. The key point here is that, within the inertial layer of the cylindrical source model, the first term of the right-hand-side of Eq. (6) dominates over the second one. This non-linear behavior of the inertia term invalidates Eq. (7) and limits the growth of $u_{\theta e}$ to $O(\sqrt{T_e/m_e})$. The same non-linear bounding mechanism is present in the 2D expansion here, so we expect it to limit the divergent growth of inertial detachment far downstream.

IV. MAGNETIC DETACHMENT

The Ampere's law (5) states that the azimuthal plasma current induces a longitudinal magnetic field \mathbf{B}^* that added to the guide field modifies the magnetic nozzle. For small-

β_0 , the induced field can be obtained by solving Eq. (5) or its integral Biot-Savart form with the zeroth order solution for j_θ . We will center the discussion in a plasma with $M \simeq 1$, $\sigma = 0$, and $\hat{\Omega}_{i0} < 1$, when the azimuthal plasma current is reduced to the Hall current developing around the plasma/vacuum edge, $J_\theta = -(p_e/B)_{r=R_V}$. This current distribution is a continuous sequence of simple loops that induces the magnetic streamfunction^{9,18}

$$\psi^*(z, r) = \frac{\mu_0}{4\pi} \int_0^{z_F} dz_1 \frac{p_e}{B_z} \sqrt{(r + R_V)^2 + (z - z_1)^2} \times [(2 - m)\mathbf{K}(m) - 2\mathbf{E}(m)] \quad (11)$$

where \mathbf{K} and \mathbf{E} are complete elliptic integrals,

$$m = \frac{4R_V r}{(r + R_V)^2 + (z - z_1)^2},$$

p_e/B_z is evaluated at $(z, r) = (z_1, R_V(z_1))$, and z_F is the length of the nozzle. The longitudinal components of the induced magnetic field satisfy $(B_z^*, B_r^*) = r^{-1}(\partial\psi^*/\partial r, -\partial\psi^*/\partial z)$, which yields

$$\hat{B}_z^*(\hat{z}, \hat{r}) = -\frac{\beta_0}{4\pi} \int_0^{z_F} d\hat{z}_1 \frac{\hat{p}_e}{\hat{B}_z} \sqrt{\frac{m}{\hat{r}\hat{R}_V}} \times \left[\mathbf{K}(m) - \frac{\hat{r}^2 - \hat{R}_V^2 + (\hat{z} - \hat{z}_1)^2}{(\hat{r} - \hat{R}_V)^2 + (\hat{z} - \hat{z}_1)^2} \mathbf{E}(m) \right], \quad (12)$$

$$\hat{B}_r^*(\hat{z}, \hat{r}) = \frac{\beta_0 \hat{z}}{4\pi \hat{r}} \int_0^{z_F} d\hat{z}_1 \frac{\hat{p}_e}{\hat{B}_z} \sqrt{\frac{m}{\hat{r}\hat{R}_V}} \times \left[\mathbf{K}(m) - \frac{\hat{R}_V^2 + \hat{r}^2 + (\hat{z} - \hat{z}_1)^2}{(\hat{r} - \hat{R}_V)^2 + (\hat{z} - \hat{z}_1)^2} \mathbf{E}(m) \right], \quad (13)$$

where the hats over the variables indicate that they have been non-dimensionalized with B_0 , $n_0 T_e$, and R . These equations show that $B_z^* B_z < 0$ and $B_r^* B_z > 0$, so that $B_z + B_z^* < B_z$ and $B_r + B_r^* > B_r$. For $\nu_{ei} \rightarrow 0$ and $m_e/m_i \rightarrow 0$, the plasma remains attached to the total magnetic nozzle, $\mathbf{B} + \mathbf{B}^*$, and therefore detaches *divergently* from the guide field.

The divergent character of the magnetic detachment is inherent to the diamagnetic character of the azimuthal plasma current in a PMN with a positive thrust gain, as the sketch of Fig. 1(a) illustrates: the counterstreaming circuit and plasma currents induce magnetic fields that oppose one to the other and reduce the total magnetic field. This increases the radial divergence of magnetic field lines. This simple argument would justify that magnetic detachment is also divergent for the more general case of $\sigma \neq 0$, when the volumetric $j_{\theta e}$ develops inside the plasma beam.

Figure 5(a) illustrates the divergent detachment of the magnetic nozzle caused by the induced field and how it increases downstream. The magnetic detachment rate is

$$\delta_{ind} = B_\perp^*/B = (B_r^* \cos \alpha - B_z^* \sin \alpha)/B, \quad (14)$$

which is, of course, proportional to β_0 . This detachment rate is plotted in Fig. 5(b) and can be compared to the diffusive detachment rates of Figs. 3(b) and 4(b). Figure 5(c) shows

how the relative strength of the induced field, $|B^*/\beta_0 B|$ increases downstream, facilitating plasma demagnetization.

The elliptic character of the Ampere's law (5) is evident in Eqs. (12) and (13): the induced field at a certain location (z, r) is determined from the plasma currents in the *whole* finite nozzle $0 \leq z \leq z_F$. Nonetheless, a plasma current loop at (z_1, r_1) influences mostly the region around it; besides, J_θ decreases downstream. Figure 5(d) plots the contributions of the set of plasma currents to $B_z^*(z, 0)$ at different axial locations; dB_z^* means the whole integrand of Eq. (12). The curves of this figure indicate that the extension of the nozzle beyond $z_F/R = 14$ will not modify the induced field for $z < z_F/2$ roughly.

The inclusion of the elliptic law (5) within our hyperbolic nozzle model would invalidate our numerical integration scheme. This does not rule out that an iterative procedure on the induced field and the plasma currents, superimposed on the hyperbolic equations for a given magnetic field, might be successful. However, a robust numerical scheme for that procedure has not been developed yet, partially because of difficulties related to the discontinuity introduced by the plasma edge and to the effect of the induced field upstream of the nozzle throat, which modifies the throat conditions. This last problem has been discussed by Ahedo recently: he analyzed, as function of β_0 , the cancelation of the axial guide field inside a cylindrical source by the diamagnetic plasma current, taking into consideration resistivity and electron inertia.¹⁹

Contrary to the case of diffusive detachment, which is always divergent, magnetic detachment is divergent as long as the diamagnetic Hall current dominates over the paramagnetic swirl current. Magnetic detachment of convergent character would take place for a cold plasma at the nozzle throat, when the Hall current is negligible but the swirl current still develops. Then, we are in the case of Fig. 1(b), when the plasma current induces a magnetic field that reinforces the guide field, leading to nozzle stretching. This conclusion agrees with the results obtained by Arefiev and Breizman¹² and Breizman *et al.*¹³

Simulations on magnetic detachment have also been performed by Winglee *et al.*² These authors adopt a multi-fluid approach with time-dependent Maxwell equations to simulate the expansion of a uniform, sonic plasma. In spite of the significant differences with the Arefiev-Breizman framework, they propose a similar detachment scenario. Seemingly their simulations show both plasma acceleration and magnetic stretching. The information they provide have not permitted us to identify the source of the disagreement with the basic (although stationary) physical principles sketched in Fig. 1.

V. FINAL DISCUSSION

The analysis of the expansion of a sonic plasma flow injected in a divergent magnetic nozzle has determined that the three detachment mechanisms proposed in the literature increase the radial divergence of the plasma plume, further hindering the efficient beam expansion to $z \rightarrow \infty$. The key physical principles for this behavior are: first, a positive

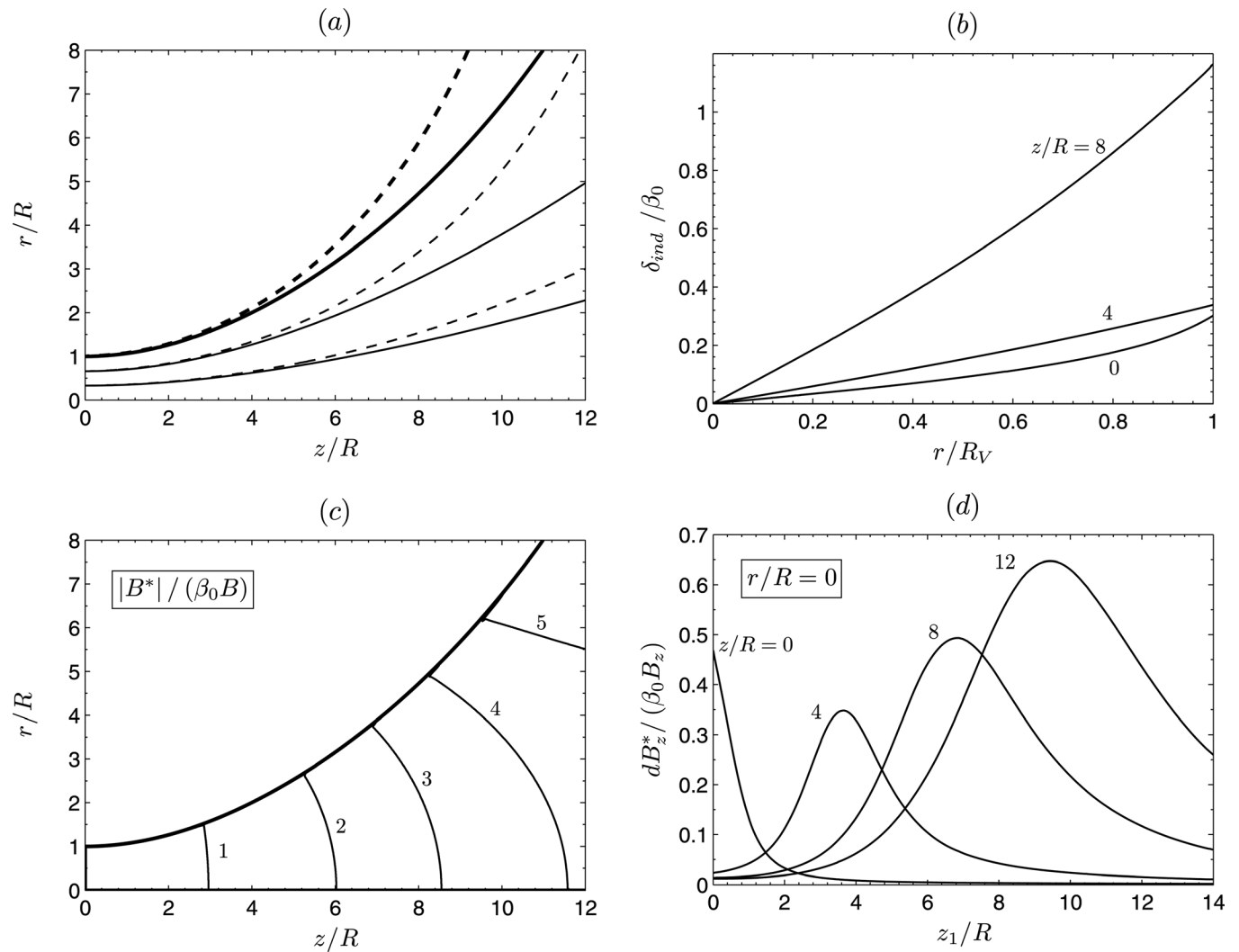


FIG. 5. Magnetic detachment for an initially uniform jet ($\sigma = 0$) and $M_0 = 1.05$, $\hat{\Omega}_{i0} = 0.1$. (a) Magnetic streamtubes for applied field (solid) total field for $\beta_0 = 0.1$ (dashed). Thick lines correspond to the plasma-vacuum edge. (b) Divergent detachment slope. (c) Map of induced-to-applied magnetic field ratio, $|B^*|/\beta_0 B$. (d) Differential induced field of the differential plasma current at $(z_1, R_V(z_1))$ on different locations $(z, 0)$ of the beam axis.

thrust gain in a PMN is intrinsically linked to the development of a diamagnetic electric current in the plasma, and second, this current always induces outward diffusion (either resistive or inertia-based) and a magnetic field that opposes the guide field and thus increases the divergence of the magnetic nozzle.

Plasma detachment was studied both qualitatively and quantitatively in terms of, on the one hand, the nozzle strength and the plasma conditions at the nozzle throat (Mach number and non-uniformity of the density profile), and on the other hand, the parameters defining the different detachment mechanisms (resistivity, electron-ion relative mass, and upstream beta parameter). The quantitative analysis was limited to the small-parameter range, but the basic physical principles explaining the plasma response support that the three detachment mechanisms will continue to be divergent in a PMN when non-linear effects account. Within our model frame, convergent detachment is limited to the induced-field mechanism and the case of a cold plasma at the nozzle throat, with no interest for propulsion applications.

The clear physical foundation of the divergent plasma response also supports that certain assumptions of our model are not contaminating the conclusions. In particular, divergent detachment of a sonic plasma beam will continue to occur under more general thermodynamic models for electrons. To this respect, a diamagnetic Hall current and a positive thrust gain have been confirmed when, instead of isothermal electrons, we implemented (1) electron cooling through a polytropic state law²⁰ and (2) a two-temperature electron population²¹ (a case observed in some studies related to helicon thrusters^{1,22–24}). As we already commented in the Introduction, the problem that still remains out of the bounds of our model is the propulsive and detachment behavior of the magnetic nozzle in the VASIMR.

Therefore, this work concludes that electron diffusion and magnetic stretching are not candidates for convergent separation of a hot plasma beam from a propulsive magnetic nozzle. Nonetheless, the analysis suggests two other basic processes as candidates for that separation, but they require extensions of the model and are left for further research. The first candidate for convergent detachment is simply *plasma*

demagnetization, which here means electron demagnetization. This is measured by the ratio ℓ_e/L_∇ , with ℓ_e and L_∇ as the local electron gyroradius and plasma gradient length, respectively. Far from the throat, we find $O(R) \leq L_\nabla \leq O(R_V)$, with $L_\nabla = O(R)$ near the plasma edge, the region where detachment would initiate. The demagnetization parameter increases rather quickly, as

$$\ell_e/L_\nabla \propto B^{-1} \propto R_V^2. \quad (15)$$

Thus, if the nozzle divergence rate is not very large, demagnetization will take place upstream of the turning point of nozzle and beam. Furthermore, in a PMN with $\beta_0 \neq 0$, the induced magnetic field favors demagnetization: indeed, B and R_V in Eq. (15) must be understood as those corresponding to the resulting magnetic nozzle. A plasma/nozzle model (either fluid or particle-based) for this scenario is not simple to build, since it must tackle with both the magnetized and the unmagnetized regions of the plasma plume.

The second candidate for convergent detachment can be termed *electrostatic separation*. To this respect, convergent ion detachment from the magnetic and electron streamtubes was already demonstrated in Ref. 9 – see Figs. 6(a) and 6(b). The ion-electron separation is enhanced when ion magnetization is decreased, which is also the optimal case for κ_{noz} and η_{plume} in a PMN. Physically, electrons follow the increasingly divergent magnetic lines, whereas ions, weakly magnetized, supersonic, and massive, are not inclined to diverge radially. This sets up a strong electric field, perpendicular to \mathbf{B} , and, associated to it, a strong rarefaction of the plasma density near the plasma edge, as Fig. 4(d) of Ref. 9 shows. In the vicinity and downstream of the nozzle turning point plasma rarefaction and electric field are going to increase sharply, and space-charge effects can matter even. Thus, even if electrons would continue to be magnetized, only a small fraction of the ion beam would turn back. The confirmation and evaluation of this detachment scenario requires a more general integration scheme, capable of extending the integration along characteristic surfaces beyond the nozzle turning point.

ACKNOWLEDGMENTS

This work has been sponsored by the Air Force Office of Scientific Research, Air Force Material Command, USAF, under grant number FA8655-10-1-3085. The U.S Govern-

ment is authorized to reproduce and distribute reprints for Governmental purpose notwithstanding any copyright notation thereon. Additional support came from the Gobierno de España (Project AYA-2010-16699). The authors thank Professor Martínez-Sánchez for his smart comments, Dr. Mitat Birkan for his support, and Ismael Martínez for helping in the computations.

¹C. Charles and R. Boswell, *Appl. Phys. Lett.* **82**, 1356 (2003).

²R. Winglee, T. Ziemba, L. Giersch, J. Prager, J. Carscadden, and B. R. Roberson, *Phys. Plasmas* **14**, 063501 (2007).

³O. Batishchev, *IEEE Trans. Plasma Sci.* **37**, 1563 (2009).

⁴D. Pavarin, F. Ferri, M. Manente, D. Curreli, Y. Guclu, D. Melazzi, D. Rondini, S. Suman, J. Carlsson, C. Bramanti, E. Ahedo, V. Lancellotti, K. Katsonis, and G. Markelov, in *Proceedings of the 31st International Electric Propulsion Conference, Ann Arbor, MI* (Electric Rocket Propulsion Society, Fairview Park, OH, 2009), paper 205.

⁵G. Krülle, M. Auweter-Kurtz, and A. Sasoh, *J. Propul. Power* **14**, 754 (1998).

⁶D. Courtney and M. Martínez-Sánchez, in *Proceedings of the 30th International Electric Propulsion Conference, Florence, Italy* (Electric Rocket Propulsion Society, Fairview Park, OH, 2007), paper 39.

⁷A. Arefiev and B. Breizman, *Phys. Plasmas* **11**, 2942 (2004).

⁸S. A. Andersen, V. O. Jensen, P. Nielsen, and N. D'Angelo, *Phys. Fluids* **12**, 557 (1969).

⁹E. Ahedo and M. Merino, *Phys. Plasmas* **17**, 073501 (2010).

¹⁰R. W. Moses, R. Gerwin, and K. Schoenberg, in *Proceedings of the Ninth Symposium on Space Nuclear Power Systems, Albuquerque, New Mexico, 1992*, AIP Conf. Proceedings No. 246, (American Institute of Physics, Woodbury NY, 1992), pp. 1293–1303.

¹¹E. B. Hooper, *J. Propul. Power* **9**, 757 (1993).

¹²A. Arefiev and B. Breizman, *Phys. Plasmas* **12**, 043504 (2005).

¹³B. N. Breizman, M. R. Tushentsov, and A. V. Arefiev, *Phys. Plasmas* **15**, 057103 (2008).

¹⁴E. Ahedo and M. Merino, in *Proceedings of the 46th Joint Propulsion Conference, Nashville, TN* (American Institute of Aeronautics and Astronautics, Washington, DC, 2010), paper 6613.

¹⁵E. Ahedo, *Phys. Plasmas* **16**, 113503 (2009).

¹⁶E. Ahedo, in *Proceedings of the 31st International Electric Propulsion Conference, Ann Arbor, MI* (Electric Rocket Propulsion Society, Fairview Park, OH, 2009), paper 193.

¹⁷A. Sasoh, *Phys. Plasmas* **1**, 464 (1994).

¹⁸J. Jackson, *Classical Electrodynamics* (Wiley, New York, 1999).

¹⁹E. Ahedo, "Beta-induced effects in a plasma confined by a cylindrical vessel and an axial magnetic field," *Phys. Plasmas* (submitted).

²⁰M. Merino, "Toberas magnéticas para motores espaciales de plasma," Engineer Degree thesis (Universidad Politécnica de Madrid, Madrid, Spain, 2010).

²¹M. Merino and E. Ahedo, in *Proceedings of the Space Propulsion 2010, San Sebastián, Spain* (European Space Agency, Noordwijk, The Netherlands, 2010), paper 1841391.

²²E. Ahedo and M. Martínez-Sánchez, *Phys. Rev. Lett.* **103**, 135002 (2009).

²³A. Sefkow and S. Cohen, *Phys. Plasmas* **16**, 053501 (2009).

²⁴E. Ahedo, *Phys. Plasmas* **18**, 033510 (2011).